

Absence of Vaccine-enhanced Disease With Unexpected Positive Protection Against severe acute respiratory syndrome coronavirus 2 (SARS-CoV-2) by Inactivated Vaccine Given Within 3 Days of Virus Challenge in Syrian Hamster Model

Can Li,^{1,a} Yan-Xia Chen,^{1,a} Fei-Fei Liu,^{1,a} Andrew Chak-Yiu Lee,^{1,a} Yan Zhao,¹ Zhan-Hong Ye,¹ Jian-Piao Cai,¹ Hin Chu,¹ Rui-Qi Zhang,¹ Kwok-Hung Chan,¹ Kelvin Hei-Yeung Chiu,² David Christopher Lung,³ Siddharth Sridhar,^{1,2} Ivan Fan-Ngai Hung,⁴ Kelvin Kai-Wang To,^{1,2} Anna Jin-Xia Zhang,^{1,a} Jasper Fuk-Woo Chan,^{1,2,5,a} and Kwok-Yung Yuen^{1,2,5,a}

¹State Key Laboratory of Emerging Infectious Diseases, Carol Yu Centre for Infection, Department of Microbiology, Li Ka Shing Faculty of Medicine, The University of Hong Kong, Pokfulam, Hong Kong Special Administrative Region, China, ²Department of Microbiology, Queen Mary Hospital, Pokfulam, Hong Kong Special Administrative Region, China, ³Department of Pathology, Queen Elizabeth Hospital, Hong Kong Special Administrative Region, China, ⁴Department of Medicine, Li Ka Shing Faculty of Medicine, The University of Hong Kong, Pokfulam, Hong Kong Special Administrative Region, China, and ⁵Hainan Medical University-The University of Hong Kong Joint Laboratory of Tropical Infectious Diseases, The University of Hong Kong, Pokfulam, Hong Kong Special Administrative Region, China.

Background. Mass vaccination against severe acute respiratory syndrome coronavirus 2 (SARS-CoV-2) is ongoing amidst widespread transmission during the coronavirus disease-2019 (COVID-19) pandemic. Disease phenotypes of SARS-CoV-2 exposure occurring around the time of vaccine administration have not been described.

Methods. Two-dose (14 days apart) vaccination regimen with formalin-inactivated whole virion SARS-CoV-2 in golden Syrian hamster model was established. To investigate the disease phenotypes of a 1-dose regimen given 3 days prior (D-3), 1 (D1) or 2 (D2) days after, or on the day (D0) of virus challenge, we monitored the serial clinical severity, tissue histopathology, virus burden, and antibody response of the vaccinated hamsters.

Results. The 1-dose vaccinated hamsters had significantly lower clinical disease severity score, body weight loss, lung histology score, nucleocapsid protein expression in lung, infectious virus titers in the lung and nasal turbinate, inflammatory changes in intestines, and a higher serum neutralizing antibody or IgG titer against the spike receptor-binding domain or nucleocapsid protein when compared to unvaccinated controls. These improvements were particularly noticeable in D-3, but also in D0, D1, and even D2 vaccinated hamsters to varying degrees. No increased eosinophilic infiltration was found in the nasal turbinate, lung, and intestine after virus challenge. Significantly higher serum titer of fluorescent foci microneutralization inhibition antibody was detected in D1 and D2 vaccinated hamsters at day 4 post-challenge compared to controls despite undetectable neutralizing antibody titer.

Conclusions. Vaccination just before or soon after exposure to SARS-CoV-2 does not worsen disease phenotypes and may even ameliorate infection.

Keywords. coronavirus; COVID-19; hamster; SARS-CoV-2; vaccine.

Received 15 January 2021; editorial decision 25 January 2021; published online 30 January 2021.

Nonstandard Abbreviations: CCL3, chemokine (C-C motif) ligand 3; CCL5, chemokine (C-C motif) ligand 5; COVID-19, coronavirus disease-2019; D-3VP, vaccinated 3 days prior; EIA, enzyme immunoassay; FFMN, fluorescence foci antibody assay microneutralization assay; IFN, interferon; IL, interleukin; IP10, interferon γ -induced protein 10; N, nucleocapsid protein; PBS, phosphate buffered saline; RBD, receptor-binding domain; RdRp, RNA-dependent RNA polymerase; RT-PCR, reverse transcription polymerase chain reaction; SARS-CoV-2, severe acute respiratory syndrome coronavirus 2; TCID₅₀, 50% tissue culture infectious doses; TNF, tumor necrosis factor; VP, inactivated SARS-CoV-2 whole virion vaccine.

^aThese authors contributed equally as co-first authors and joint last authors.

Correspondence: K.-Y. Yuen, State Key Laboratory of Emerging Infectious Diseases, Carol Yu Centre for Infection, Department of Microbiology, Li Ka Shing Faculty of Medicine, The University of Hong Kong, 102 Pokfulam Road, Pokfulam, Hong Kong Special Administrative Region, China (kyuen@hku.hk).

Clinical Infectious Diseases® 2021;73(3):e719–34

© The Author(s) 2021. Published by Oxford University Press for the Infectious Diseases Society of America. This is an Open Access article distributed under the terms of the Creative Commons Attribution-NonCommercial-NoDerivs licence (<http://creativecommons.org/licenses/by-nc-nd/4.0/>), which permits non-commercial reproduction and distribution of the work, in any medium, provided the original work is not altered or transformed in any way, and that the work is properly cited. For commercial re-use, please contact journals.permissions@oup.com
DOI: 10.1093/cid/ciab083

The coronavirus disease-2019 (COVID-19) pandemic caused by the emerging severe acute respiratory syndrome coronavirus 2 (SARS-CoV-2) has affected over 90 million people, with about 2 million deaths after 1 year [1]. The high transmissibility of SARS-CoV-2 is attributable to the high viral loads in respiratory specimens at or just before the time of symptom onset [2], which accounts for high attack rates in indoor settings [3–5], and is likely mediated through short-range aerosol transmission in addition to droplet and contact transmission. Although only 15% of SARS-CoV-2 reverse transcription polymerase chain reaction (RT-PCR)-positive cases develop severe disease leading to respiratory failure [6], the high incidence of COVID-19, especially during winter, has placed enormous burden on healthcare services in many affected areas. While patients with milder disease may be monitored and isolated at home, respiratory support and intensive care treatment are reserved for those hospitalized with severe disease. Unfortunately, monotherapy

with repurposed antiviral agents, such as remdesivir, lopinavir-ritonavir, interferon beta, and hydroxychloroquine have little or no effect in hospitalized COVID-19 patients with severe disease [7, 8]. Monoclonal antibody cocktails may reduce rates of hospitalization and hasten clearance of viral load when given in early disease, but do not alter outcomes in patients with severe COVID-19 [9, 10]. Similarly, treatment with convalescent plasma in randomized clinical trials only improved the clinical status of elderly with mild COVID-19 when given within 3 days of symptom onset, and was not effective after hypoxemia developed [11, 12]. Therefore, before sufficient herd immunity is built up by vaccination, strict border controls, social distancing which severely affect schooling, traveling, mental health, and socioeconomic activities, extensive testing for case identification and isolation, painstaking contact tracing and quarantine, universal masking and better hand hygiene remain on the long list of expensive, labor intensive and difficult-to-implement epidemiological measures to reduce morbidity and mortality of the COVID-19 pandemic [13].

While mRNA, chimpanzee adenovirus vectored, and inactivated whole virion SARS-CoV-2 vaccines have recently been approved for emergency use in different countries, there are still concerns about the possibilities of vaccine-enhanced disease or antibody-dependent enhancement of disease [14]. Preclinical studies in experimental animals including nonhuman primates have so far not demonstrated such deleterious complications when the virus challenge was given weeks after a full course of vaccination [15–17]. However, data on the outcomes when the vaccine is given in close temporal juxtaposition to SARS-CoV-2 infection, when vaccine-induced antibodies are still undetectable or of low avidity, are not available. Vaccine-enhanced diseases were reported in patients who developed atypical measles or severe respiratory syncytial virus infection after being given formalin-inactivated whole virion vaccines which induce a T helper-2 immune response with relatively low levels of poorly neutralizing antibodies of poor avidity [18, 19]. Moreover, antibody-dependent enhancement of disease was suspected to worsen SARS-CoV-1 and other virus infections [20].

We have previously established a golden Syrian hamster model which simulates the clinical manifestations of COVID-19 in humans [5]. In this study, we analyzed the serial clinical scores, body weight loss; lung and nasal turbinate viral loads and infectious virus titer; tissue virus antigen expression, histopathology score, gene expression level of cytokines and chemokines; and antibody response of hamsters vaccinated with formalin inactivated whole SARS-CoV-2 virion 3 days before, 1 to 2 days after, and on the day of virus challenge.

MATERIALS AND METHODS

SARS-CoV-2 Virus and Inactivated Whole Virion Vaccine

SARS-CoV-2 HK-13 strain (GenBank accession number: MT835140) was cultured and titrated in African green monkey

kidney cells (Vero E6) [21]. To prepare inactivated SARS-CoV-2 whole virion vaccine, SARS-CoV-2 HK-13 inoculated Vero E6 cell culture supernatant collected at 72 hours postinoculation was inactivated with 0.1% (v/v) formalin at 4°C for 7 days. The efficiency of inactivation was determined by plaque forming assay on Vero E6 cells as described [22]. The inactivated virus was then purified and concentrated by sucrose gradient ultracentrifugation at 28 000 rpm [23]. Collected inactivated virus was tested for total protein amount by bicinchoninic acid protein assay (Thermo Fisher Scientific) (Supplementary Materials).

Animals

Male and female Syrian hamsters at 6–8 weeks of age were obtained from the Chinese University of Hong Kong Laboratory Animal Service Centre through the HKU Centre for Comparative Medicine Research. The animals were kept in BSL-2 animal facility with 12-hour light-dark cycle and free access to feed and water [24]. All the animal experimental procedures were approved by the Committee on the Use of Live Animals in Teaching and Research of HKU.

Vaccination Procedure

The hamsters were randomly divided into groups. For demonstration of protection by formalin-inactivated whole virion vaccine given at usual timing, a 2-dose-regimen of vaccination at 14 days apart (10 µg of total protein in 100 µL/dose) was given as indicated in Figure 1A. For the evaluation of the effect of vaccination close to the time of virus challenge, a 1-dose-regimen of vaccination was given 3 days prior to (D-3), immediately before (D0) virus challenge, 1 day or 2 days after virus challenge (D1 and D2, respectively). Animals in control groups were injected with same volume of phosphate buffered saline (PBS) (Supplementary Materials).

SARS-CoV-2 Challenge

To demonstrate vaccine-induced protection, the hamsters were intranasally inoculated with 50 µL of PBS-diluted SARS-CoV-2 (1×10^3 PFUs) at 14 days after the second dose of vaccination. This higher virus inoculum was used to check the degree of protection after the 2-dose-regimen. To demonstrate the effect of 1-dose-regimen of vaccine given just before or after virus challenge, a lower virus inoculum of 50 PFUs of SARS-CoV-2 (HK-13) was intranasally inoculated to achieve a better differentiation of the low level protection induced by such a short interval between vaccination and virus challenge. Body weight and clinical signs of diseases were monitored for 4 to 14 days postchallenge. At day 4 postchallenge (4 dpi) when disease is usually severe, 3 hamsters from each group were sacrificed. The nasal turbinate, lung, small intestine, and serum samples were collected for virological and histopathological studies. All experiments

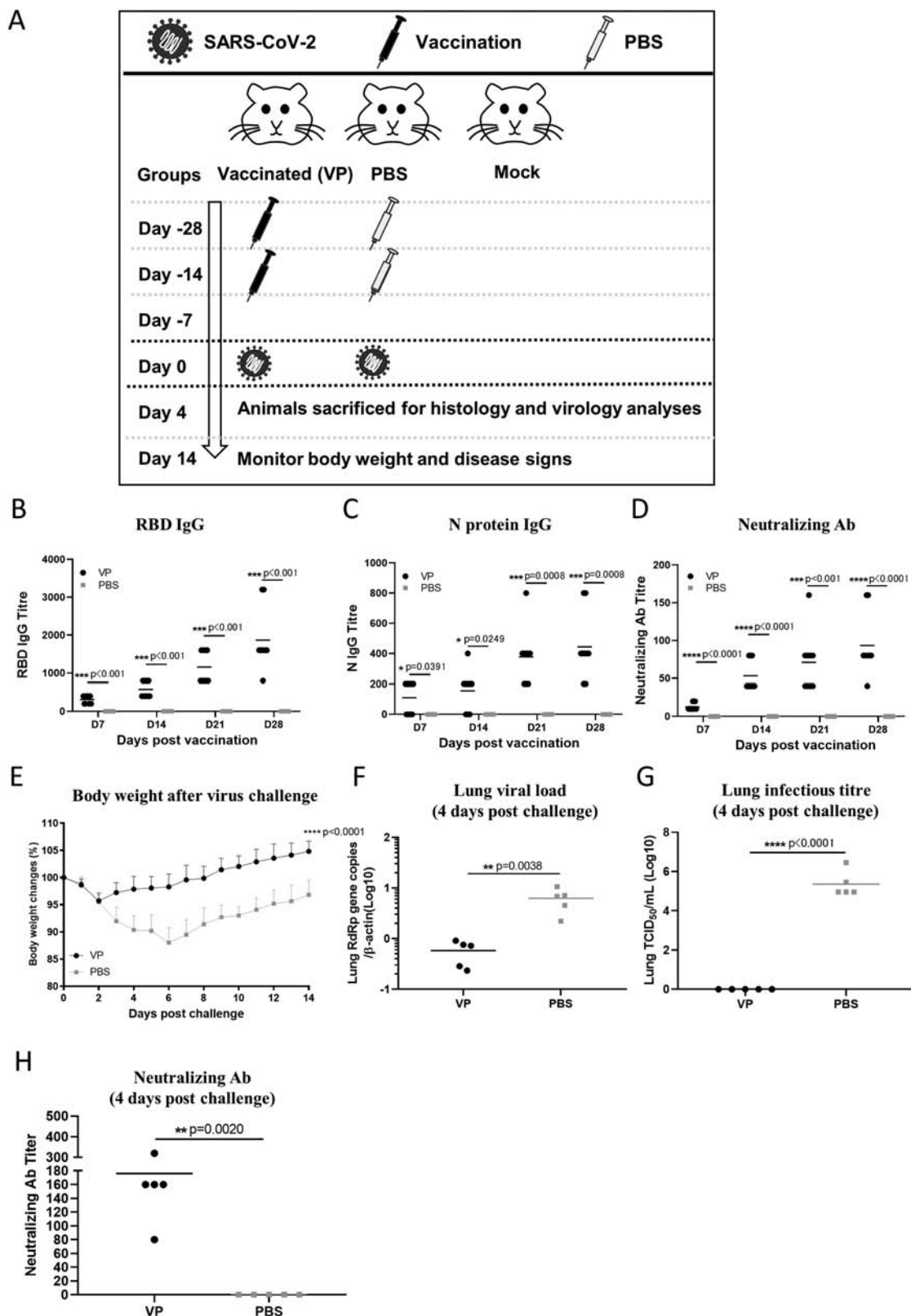


Figure 1. A. Schematic representation of the schedule of vaccination with inactivated SARS-CoV-2 whole virion vaccine, vaccine-induced serum antibody response, and protection from virus challenge in the golden Syrian hamster model. Two-dose-regimen vaccination demonstrated protection. Syrian hamsters at 6–8 weeks of ages were randomly divided into groups. Formalin-inactivated SARS-CoV-2 whole virion vaccine containing 10 μ g of total protein in 100 μ L was administered at a 14-day interval. The control animals received the same volume of PBS as the vaccinated animals. Blood samples were collected at days 7, 14, 21, and 28 after the first dose of vaccination for antibody determination. Virus challenge was performed at day 14 after the second dose of vaccination. At day 4 postvirus challenge (4 dpi), 3 animals in each group were

involving live SARS-CoV-2 virus were carried out in a bio-safety level 3 laboratory.

Virological, Histopathological, Immunological, and Serological Analyses of Samples Collected at 4 Days Post-virus Challenge

The methods for determination of lung and nasal turbinate tissue viral load by quantitative real-time reverse transcriptase-polymerase chain reaction (qRT-PCR), 50% tissue culture infectious doses (TCID₅₀) assay, mRNA expression levels for cytokines and chemokines in lung homogenates [25, 26], microneutralization antibody assay [27], and single-cycle virus inhibition fluorescence foci microneutralization antibody (FFMN) assay [28], detection of viral antigen specific IgG in hamster serum by enzyme immunoassay (EIA) [2], histopathology scoring and immunofluorescence staining were performed as we previously described and elaborated in [Supplementary Materials](#).

Statistical Analysis

All data were analyzed with Prism 8.0 (GraphPad Software Inc). One-way ANOVA, Student's *t*-test, or Mann-Whitney test were used to determine the significance of differences among different groups as stated in figure legends. *P* < .05 was considered statistically significant.

RESULTS

Two-dose Vaccination Regimen with Inactivated SARS-CoV-2 Vaccine Induced Serum Neutralizing Antibody and Protected Hamster from Virus Challenge

To validate the standard 2-dose-regimen of the formalin-inactivated SARS-CoV-2 whole virion vaccine in the hamster model, we showed that the regimen induced serum IgG antibody against SARS-CoV-2 spike receptor-binding domain (RBD) and nucleocapsid (N) protein, which correlated with the rising neutralizing titer from day 7 to day 28 after first vaccination ([Figure 1B–1D](#)). Good protection against intranasal challenge by 10³ PFUs of SARS-CoV-2 14 days after the second dose vaccination was evidenced by a significantly lower body weight loss, lower lung viral load, and undetectable infectious virus titer at day 4 postchallenge (4 dpi) than the PBS control ([Figure](#)

[1E–1G](#)), and a fast raising high titer of serum neutralizing antibody detected at 4 dpi ([Figure 1H](#)). Notably, a limited amount of immunofluorescent N antigen expression was still found in the lungs of vaccinated hamsters ([Figure 2A](#)). However, the pulmonary inflammatory infiltrates were only mild and confined to the alveolar wall ([Figure 2B](#)). In terms of cytokine and chemokine expression in lung, vaccinated hamsters had significantly higher interferons (IFN- α , IFN- γ), interleukin 6 (IL-6), tumor necrosis factor (TNF- α), whereas the PBS control had a significantly higher interferon γ -induced protein 10 (IP-10) and chemokine (C-C motif) ligand 5 (CCL5) ([Figure 2C](#)). As expected, the histopathological changes of intestinal inflammation, epithelial necrosis, and submucosal edema were much less severe in vaccinated hamsters than in PBS controls ([Figure 2D](#)).

As for the upper respiratory tract, the viral load in nasal turbinate was significantly reduced in vaccinated hamsters by half a log compared to PBS controls ([Figure 3A](#)), no detectable infectious titer, with decreased inflammation, mucosal necrosis and detachment, and immunofluorescent N expression ([Figure 3B](#) and [3C](#)). Serial viral loads in oral swabs were reduced in the vaccinated hamsters, unlike the PBS controls which were still above cut-off between day 8 to day 12 postchallenge ([Figure 3D](#)).

One-dose Vaccination 3 Days Prior or Immediately Before Virus Challenge Accelerated Neutralizing Antibody Production and Reduced the Disease Severity in Hamster

When hamsters were vaccinated 3 days prior to (D-3VP) or immediately before SARS-CoV-2 challenge (D0 VP) ([Figure 4A](#)), the clinical scores of disease severity were significantly lower in D-3 and D0 vaccinated hamsters ([Table 1](#)). Their weight loss was generally less than the PBS controls though not reaching statistical significance ([Figure 4B](#)). Interestingly, viral loads of harvested lung and nasal turbinate at 4 dpi were significantly lower in D-3 vaccinated hamsters than in PBS controls ([Figure 4C](#)). Furthermore, infectious titers in nasal turbinates and lungs were significantly lower in the D-3 vaccinated and even the D0 vaccinated hamsters ([Figure 4D](#)). These findings were compatible with lower histology score with less severe inflammation, little vasculitis, and lower amount of N expression in the lungs of D-3 and D0 vaccinated hamsters ([Figure 4E](#) and [4F](#); [Table 1](#)).

sacrificed for virological and histopathological analyses. The remaining animals were monitored for 14 days postvirus challenge. *B*. Serum IgG titer against the SARS-CoV-2 spike protein receptor-binding domain (RBD) was determined by enzyme immunoassay (EIA) at different times after vaccination. *n* = 9 for the vaccine and *n* = 5 for PBS control groups at each time point. *C*. Serum IgG titer against SARS-CoV-2 nucleocapsid (N) protein was determined by EIA at different times after vaccination. *n* = 9 for the vaccine and *n* = 5 for PBS control groups at each time point. *D*. Serum neutralizing antibody titer against SARS-CoV-2 was determined by microneutralization test in Vero E6 cells. *n* = 9 for the vaccine and *n* = 5 for PBS control groups at each time point. Error bars indicated standard deviations. *P* values were calculated Student's *t*-test. *E*. Body weight changes after virus challenge. At 14 days after second dose of vaccination, the hamsters were intranasally challenged with 10³ PFUs of SARS-CoV-2. Body weight was monitored for 14 days. *n* = 5 for the vaccine group and *n* = 4 for the PBS control group. *F*. qRT-PCR was used to determine the viral load in hamster lung homogenates at 4 post-virus challenge. *n* = 5 for the vaccine group and *n* = 5 for the PBS control group. Error bars indicated standard deviations. *P* values were calculated by Student's *t*-test. *G*. Infectious virus titer in the lung samples collected at 4 days post virus-challenge was determined by 50% tissue culture infectious dose (TCID₅₀) assay in Vero E6 cells. *n* = 5 for the vaccine group and *n* = 5 for the PBS control group. Error bars indicated standard deviations; *P* values were calculated by Student's *t*-test. *H*. Neutralizing antibody titer against SARS-CoV-2 in the sera obtained at 4 days post virus-challenge (4 dpi). *n* = 5 for the vaccine group and *n* = 5 for the PBS control group. The error bars indicated standard deviations. *P* values were calculated by Student's *t*-test. The data presented were from 2 independent experiments. Abbreviations: EIA, enzyme immunoassay; N, SARS-CoV-2 nucleocapsid protein; RBD, SARS-CoV-2 spike protein receptor-binding domain; RdRp, SARS-CoV-2 RNA-dependent RNA polymerase; VP, inactivated SARS-CoV-2 whole virion vaccine.

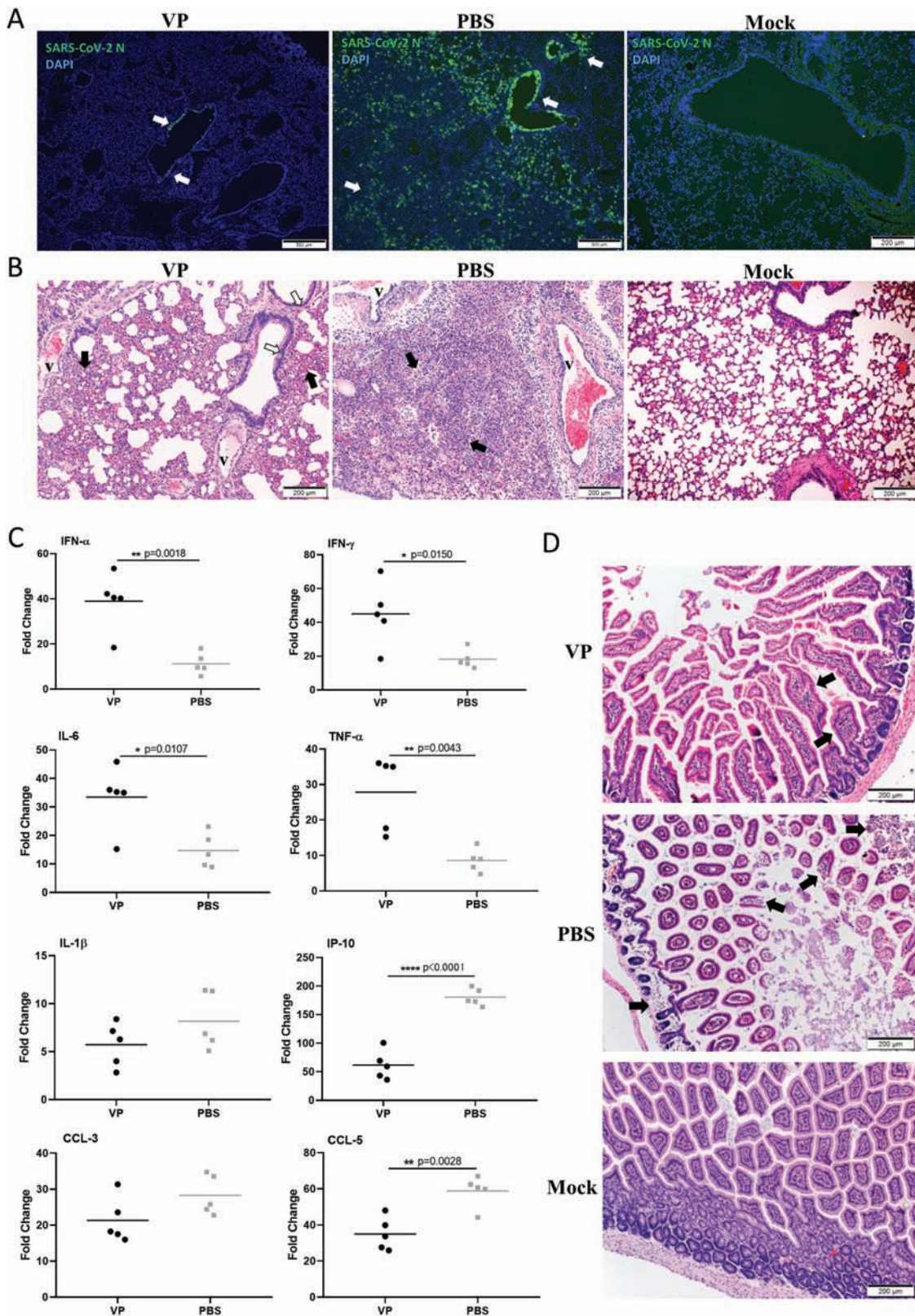


Figure 2. Histopathological changes in the lung and small intestine of the hamsters at 4 days post virus-challenge (4 dpi). The hamsters were vaccinated with 2 doses of inactivated SARS-CoV-2 whole virion vaccine or phosphate-buffered saline (PBS; control). The animals were challenged with 10^3 PFUs of SARS-CoV-2 at 14 days after the second dose of vaccine. The lung, nasal turbinate, and intestine were sampled at 4 dpi. **A.** Representative images of immunofluorescence-stained SARS-CoV-2 nucleocapsid protein (N) in the hamster lung tissue sections. Small foci of N-expressing cells were shown in the lungs of the vaccinated hamsters (VP, arrows), while diffuse alveolar distribution of N protein was observed in the lungs of the control hamsters mock-vaccinated with PBS. Scale bars = 500 μ m for vaccinated and control hamsters and 200 μ m for

The inflammatory infiltrate was largely mononuclear cells with no excess eosinophils. As for the expression levels of cytokines and chemokines in lung, significantly higher IFN- α , IFN- γ , IL-1 β , and CCL5 were found in D-3 vaccinated and sometimes also D0 vaccinated hamsters, but not IP-10 (Figure 4G). Notably, at 4 dpi, serum neutralizing antibody and IgG against SARS-CoV-2 Spike RBD and N were significantly higher in D-3 vaccinated than D0 vaccinated hamsters and PBS control (Figure 4H). Using a highly sensitive single-cycle virus inhibition FFMN assay, these 4dpi-sera from D-3 and D0 vaccinated hamsters neutralized SARS-CoV-2 with significant reduction of N-antigen positive fluorescent foci in Vero E6 cells compared to PBS controls (Figures 4I and 4J).

One-dose Vaccination One or Two Days After Virus Challenge Showed Beneficial But No Detrimental Effect in Hamster

When vaccination was given 1 day (D1VP) or 2 days (D2VP) after virus challenge, vaccinated hamsters had less weight loss, though not reaching statistical significance (Figure 5A). The viral load of nasal turbinate on day 4 post-challenge of D1 vaccinated hamsters was significantly lower than PBS control, but no significant differences for lung viral load (Figure 5B). More importantly, lung and nasal turbinate showed significantly lower infectious titers in the D1 vaccinated hamsters. Even the D2 vaccinated hamster showed a lower nasal turbinate infectious titer than PBS control (Figure 5C). The expression levels of IFN- α and IFN- γ were significantly higher in the lung of D1 vaccinated hamsters, whereas CCL3 and IP-10 were significantly higher in PBS control (Figure 5D). The lung histology scores (Table 1), inflammatory infiltration, and immunofluorescent N expression were not significantly different (Figure 5E and 5F). No excess eosinophils were noted in the inflammatory infiltrates. Interestingly, serum IgG titers against RBD and N in D1 and D2 vaccinated hamsters were significantly higher than PBS controls (Figure 5G) on day 4 postchallenge. These sera significantly reduced N-positive fluorescent foci by FFMN assay (Figure 5H and 5I) despite undetectable titer by conventional neutralization assay. This finding shows that the humoral antibody response observed is due to the vaccine rather than the virus challenge.

As for extra-pulmonary tissue, the degree of intestinal inflammation, epithelial necrosis, submucosal edema, and N

antigen expression appeared to be highest in the PBS controls, followed by D2, D1, D0, and D3 vaccinated hamsters, respectively (Figure 6).

DISCUSSION

Vaccination of hamsters with conventional 2-dose-regimen of formalin-inactivated whole virion before virus challenge induced good neutralizing antibody response and protected fully against SARS-CoV-2. Even the 1-dose-regimen given within 3 days of SARS-CoV-2 challenge did not result in any vaccine-enhanced diseases. Notably, the vaccinated hamsters had significantly less severe clinical scores and lung histology scores, lower infectious virus titers in lung or nasal turbinate, less N antigen expression, less inflammatory changes in intestines, and a higher serum neutralizing antibody or IgG titer against RBD or N. These findings were particularly noticeable in D-3 vaccinated hamsters, but also at various degrees in D0, D1, and even D2 vaccinated hamsters. No increase in eosinophilic infiltration in nasal turbinate or lung was noted after virus challenge.

The effect of whole population vaccination against coronavirus infection is completely unknown to mankind. While the benefit of vaccination is likely to outweigh the physical and psychosocial morbidity, mortality, and economic disruption of the COVID-19 pandemic, some unexpected risks of coronavirus vaccines have to be addressed to reassure the general public. Besides rare complications such as anaphylaxis against vaccine excipients such as polyethylene glycol, or immunopathology such as transverse myelitis, potential threats are vaccine-enhanced diseases which have happened with formalin-inactivated whole virion vaccines for measles and respiratory syncytial virus [18, 19]. Another possibility is antibody-dependent disease enhancement, which has been implicated in dengue and SARS-CoV-1 vaccines [20, 29]. Such complications are particularly implicated in vaccines which induce a T-helper 2 response with antibodies having low avidity and poorly neutralizing activity. This situation is possible with inactivated whole virion SARS-CoV-2 vaccines, especially when individuals are exposed to the wild-type virus before completing the whole course of the vaccine. Though vaccination studies with nonhuman primates did not show such vaccine-enhanced diseases with mRNA, adenoviral vector, or

the mock-infected hamsters. *B.* H&E images of the lung tissue sections at 4 dpi. In the lungs of the vaccinated hamsters (VP), the solid arrows indicated increased thickness of the alveolar wall. No obvious epithelial cell death or luminal debris in the bronchioles was observed (open arrows). The 2 sections of blood vessels ("v") show no vasculitis. The lungs of the PBS control hamsters (PBS) showed diffuse alveolar wall and alveolar space infiltration by inflammatory cells (solid arrows). Severe inflammatory cell infiltration in the wall and endothelium of the two blood vessels ("v") were observed. Scale bars = 200 μ m. *C.* Gene expression profile of inflammatory cytokines/chemokines in the lung tissues of the hamsters at 4 dpi determined by qRT-PCR. The relative expression levels of each gene compared to mock-infected hamsters were shown. *n* = 5 for the vaccine group and *n* = 5 for the control PBS control group. The error bars indicated standard deviations. *P* values were calculated by Student's *t*-test. *D.* H&E images of small intestine sections of the hamsters at 4 dpi. The intestines of the vaccinated hamsters (VP) showed mild degree of inflammatory infiltration and congestion at the intestinal lamina propria, but the intestinal villi were intact (arrows). The intestines of the control hamsters showed severe edema and inflammatory infiltration at the lamina propria, and destruction of some of the intestinal villi (solid arrows). The data presented were from 2 independent experiments. Abbreviations; CCL3, chemokine (C-C motif) ligand 3; CCL5, chemokine (C-C motif) ligand 5; DAPI, 4',6-diamidino-2-phenylindole; IFN- α , interferon alpha; IFN- γ , interferon gamma; IL-1 β , interleukin 1 beta; IL-6, interleukin 6; IP-10, interferon gamma induced protein 10; N, SARS-CoV-2 nucleocapsid protein; TNF- α , tumor necrosis factor alpha; VP, inactivated SARS-CoV-2 whole virion vaccine.

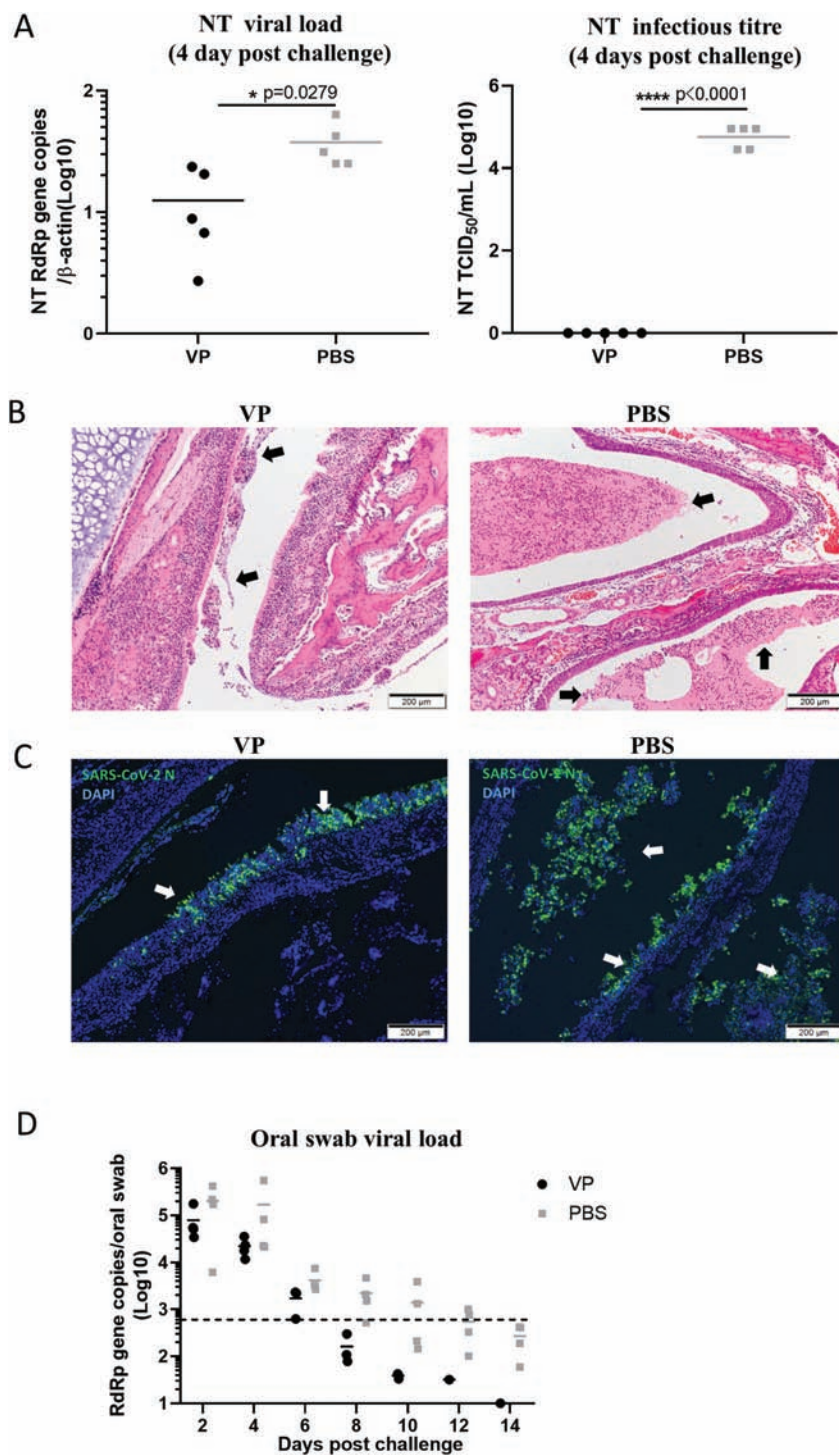


Figure 3. Viral load and histopathology of nasal turbinate of the hamsters at day 4 post-virus challenge. **A.** The viral load in the nasal turbinate tissue homogenates was determined by qRT-PCR (left panel). Right panel, infectious viral titer in nasal turbinate homogenates determined by 50% tissue culture infectious dose (TCID₅₀) assay in Vero E6 cells. $n = 5$ for the vaccine group and $n = 5$ for the PBS control group. The error bars indicated standard deviations. P values were calculated by Student's t -test. **B.** Representative H&E images of the nasal turbinate of the hamsters. The nasal turbinate sections of the vaccinated hamsters (VP) showed an intact epithelial layer, with some degree of intra-epithelial and submucosal inflammatory cell infiltration. Luminal secretion and cell debris were observed in focal areas (arrows). In contrast, the nasal turbinate sections of the PBS control hamsters showed massive secretion and cell debris filling the lumen (arrows). Scale bars = 200 μ m. **C.** Representative images of immunofluorescence-stained SARS-CoV-2 nucleocapsid (N) protein in nasal turbinate tissues at 4 dpi. Focal nasal turbinate epithelium in the vaccinated hamsters (VP) showed markedly less viral N protein expression (arrows) than the PBS control hamsters, in which, most of the N-positive cells being detached and found inside the nasal cavity (arrows). Scale bars = 200 μ m. **D.** Viral load in the oral swabs collected from vaccinated (VP) or PBS control (PBS) hamsters every other day during the 14 days post virus-challenge. The SARS-CoV-2 RdRp gene copy number was determined by qRT-PCR. The dashed line indicated the detection limit. The data presented were from 2 independent experiments. Abbreviations: DAPI, 4',6-diamidino-2-phenylindole; N, SARS-CoV-2 nucleocapsid protein; NT, nasal turbinate; RdRp, SARS-CoV-2 RNA-dependent RNA polymerase; VP, inactivated SARS-CoV-2 whole virion vaccine.

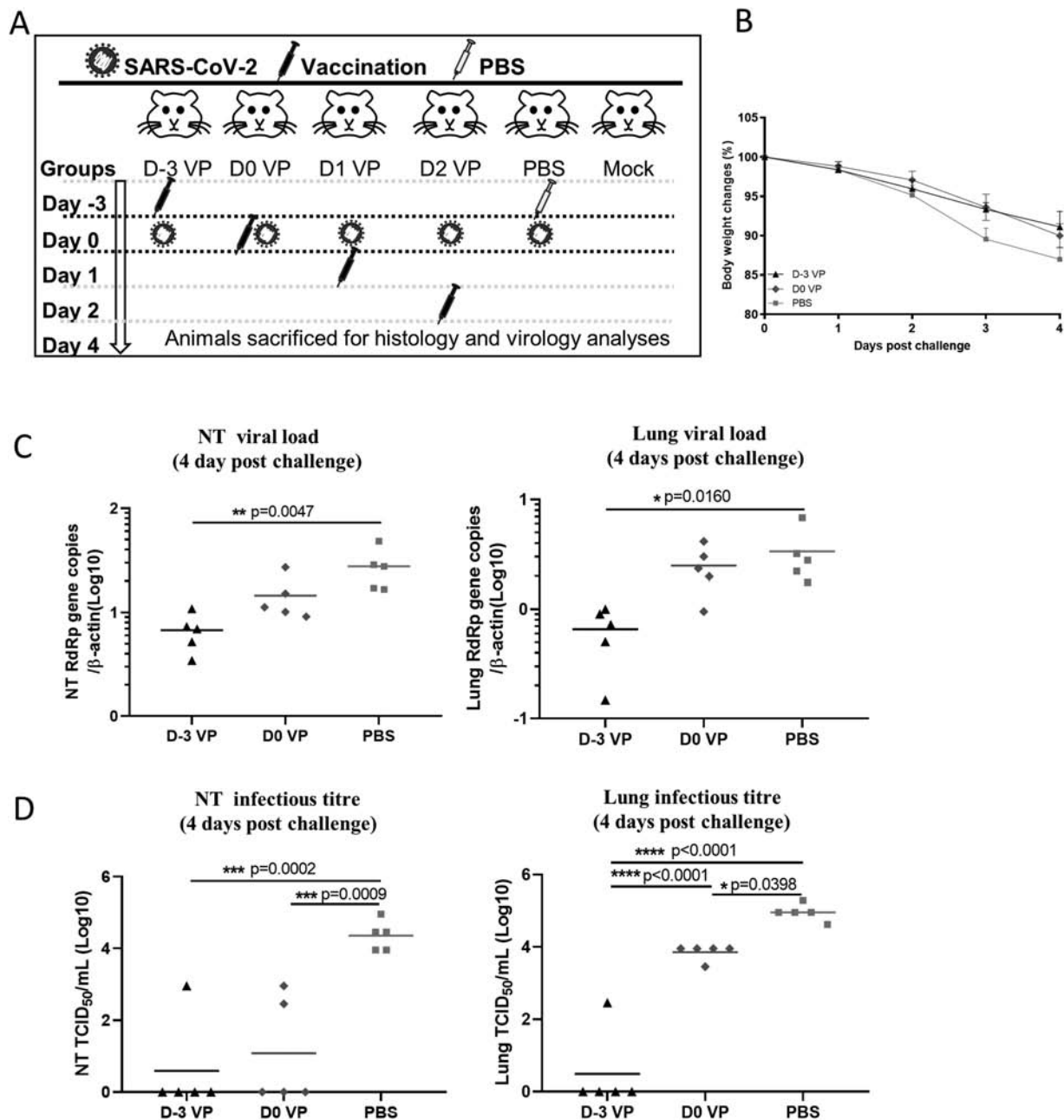


Figure 4. The outcomes of the hamsters which received vaccination at 3 days before or immediately before virus challenge. **A.** Schematic representation of the vaccination schedule using a 1-dose vaccination regimen at different times before or after virus challenge. The same dose of formalin-inactivated SARS-CoV-2 vaccine (10 μ g total protein) as in the 2-dose regimen was used to vaccinate the hamsters 3 days before, immediately before, and 1 day or 2 days after virus challenge. The animals were monitored for 4 days and sacrificed for analysis at 4 dpi. **B.** Body weight changes of the hamsters during the 4-day observation period after virus challenge. $n = 5$ for each group. The error bars indicated standard deviations. **C.** The viral load in the hamsters' nasal turbinates (left) and lung (right) tissues at 4 dpi were determined by qRT-PCR. $n = 5$ for each group. The error bars indicated standard deviations. P values were calculated by one-way ANOVA. **D.** The infectious viral titer in the hamsters' nasal turbinates (left) and lung (right) tissues at 4 dpi was determined by TCID₅₀ assay in Vero E6 cells. $n = 5$ for each group. The error bars indicated standard deviations. P values were calculated by one-way ANOVA. **E.** Representative H&E-stained images of the hamsters' lung tissues at 4 dpi. The lung sections of the hamsters vaccinated at 3 days before virus challenge (D-3 VP) showed peribronchiolar ("b") inflammatory infiltration with little luminal debris. A focal area with inflammatory infiltration in the alveolar space (arrows) and mild degree of vascular wall infiltration ("v") were observed. The lung sections of the hamsters vaccinated immediately before virus challenge (D0 VP) showed severe inflammatory infiltration in a blood vessel ("v"), and less alveolar exudation and infiltration as those in the PBS control hamsters. Scale bars = 200 μ m. **F.** Representative immunofluorescence-stained images of viral N protein in the hamsters' lung tissues at 4 dpi. In the D-3 vaccinated hamsters (D-3 VP), SARS-CoV-2 N protein expression ("N") was mainly found in the bronchiolar epithelium (arrows), whereas in the D0 vaccinated hamsters (D0 VP), the alveoli adjacent to the bronchiole also showed viral N protein expression (arrows). More extensive N protein expression was found in the lungs of the PBS control hamsters. Scale bars = 200 μ m. **G.** Gene expression profile of inflammatory cytokines/chemokines in the lung tissues of the hamsters at 4 dpi determined by qRT-PCR. The relative expression levels of each gene compared to mock-infected hamsters were shown. $n = 5$ for each group. The error bars indicated standard deviations. P values were calculated by Student's t -test. **H.** Serum IgG titre against RBD (left panel) and N protein (middle) at 4 days post virus-challenge were determined by enzyme immunoassay (EIA). The right panel showed the serum neutralizing antibody titer determined by microneutralization assay in Vero E6 cells. $n = 5$ for each group. The error bars indicated standard deviations. P values were calculated by Mann-Whitney

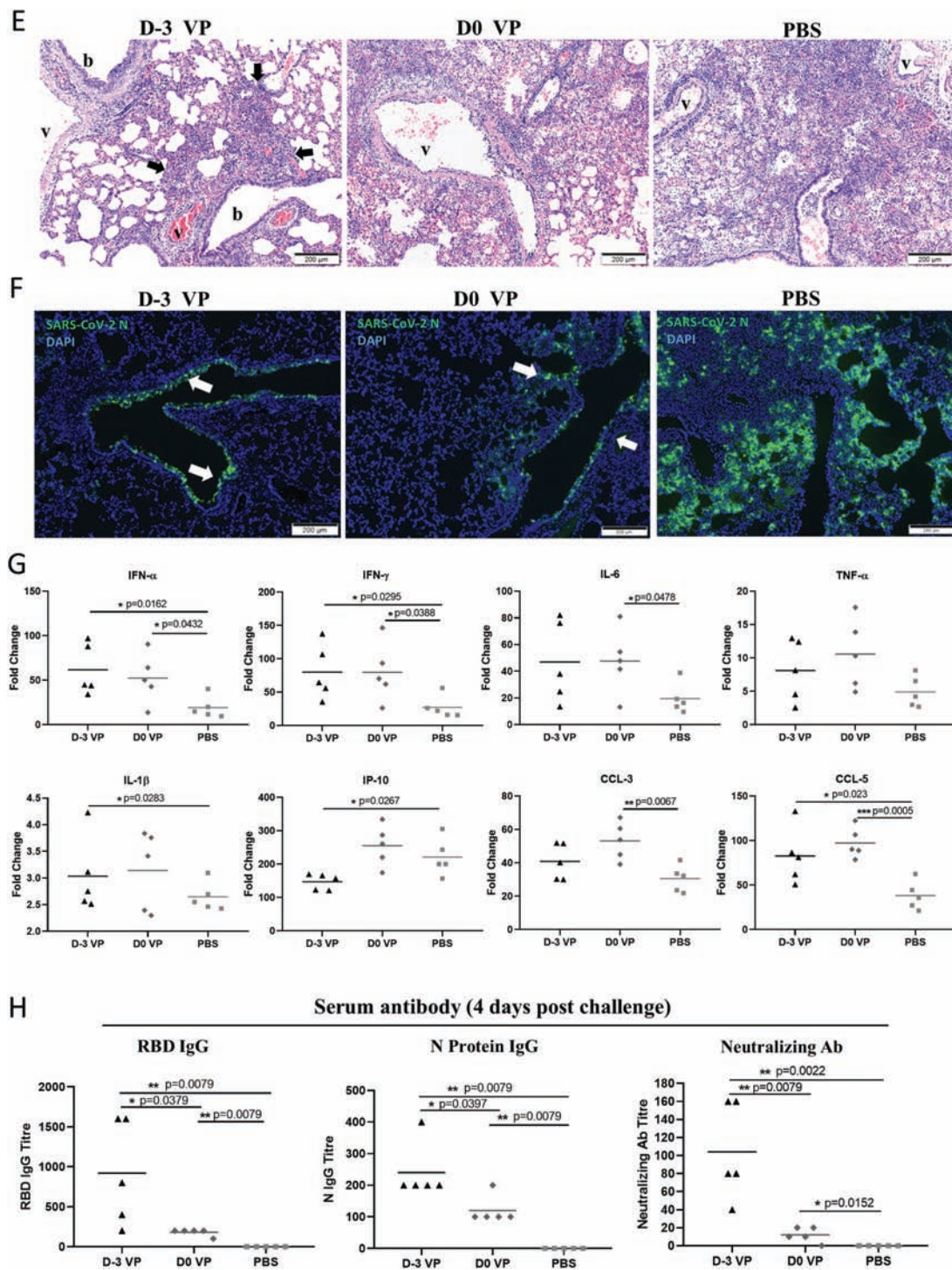


Figure 4. Continued.

test. *I*. Representative images of immunofluorescence-stained SARS-CoV-2 N protein in FFMN assay using Vero E6 cells. SARS-CoV-2 (MOI = 0.1) was allowed to react with the diluted sera obtained from the hamsters vaccinated at D-3 or D0, or PBS control hamsters for 1 hour at 37°C before being added to Vero E6 cells. The cells were then fixed and stained for SARS-CoV-2 N protein after 6 hours of incubation. Mock-infected hamster serum samples were tested in parallel as control. *J*. Percentage of reduction of N-positive cell by vaccinated hamsters' sera versus PBS control hamster sera in FFMN assay. $n = 3$ for each group. *P* values were calculated by Student's *t*-test. The data presented were from 2 independent experiments. Abbreviations: CCL3, chemokine (C-C motif) ligand 3; CCL5, chemokine (C-C motif) ligand 5; DAPI, 4',6-diamidino-2-phenylindole; dpi, day post virus challenge; FFMN, fluorescence foci microneutralization; IFN- α , interferon alpha; IFN- γ , interferon gamma; IL-1 β , interleukin 1 beta; IL-6, interleukin 6; IP-10, interferon gamma induced protein 10; N, SARS-CoV-2 nucleocapsid protein; NT, nasal turbinate; RBD, SARS-CoV-2 spike protein receptor binding domain; RdRp, SARS-CoV-2 RNA-dependent RNA polymerase; TNF- α , tumour necrosis factor alpha; VP, inactivated SARS-CoV-2 whole virion vaccine.

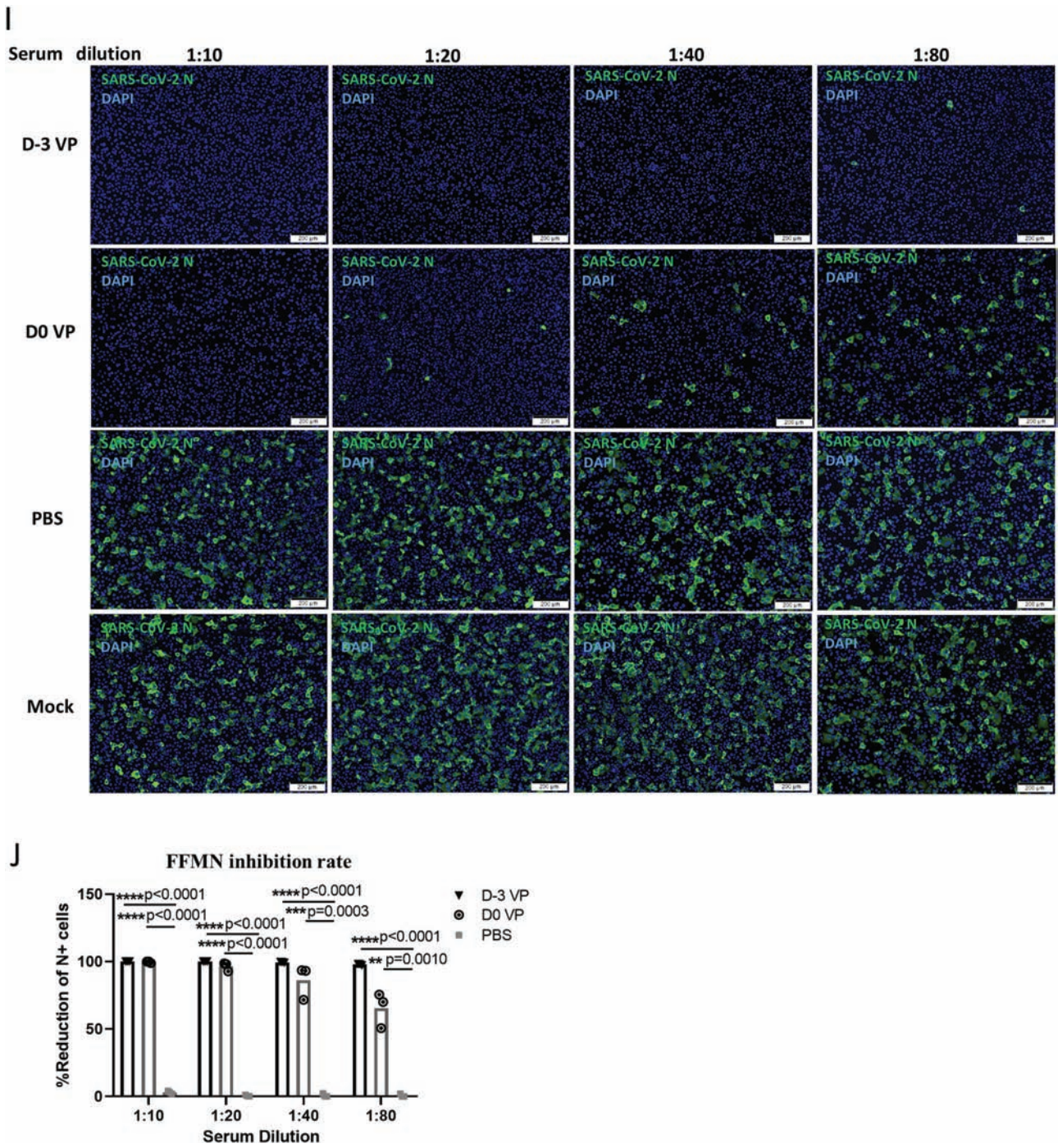


Figure 4. Continued.

inactivated whole virion SARS-CoV-2 vaccines, the interval between first dose of vaccination to virus challenge spanned over 3 to 8 weeks, which allows the mounting of a good adaptive immune response after affinity maturation of antibody. However, no data on the effect of a single dose of vaccine given within a few days before or after virus challenge are available. In this study, the formalin-inactivated whole virion vaccine was chosen for further evaluation in the hamster model because

this vaccine is known to induce a T-helper 2 response with little CD8 cytotoxic or CD4 cell-mediated immunity [15], unlike the mRNA [17] or adenoviral vector vaccines [16] which induced a T helper 1 response with significant CD8 and CD4 lymphocyte mediated immunity.

Vaccine-enhanced disease was not found in our hamster model when the inactivated vaccine was given within a few days before or after virus challenge when antibody affinity maturation

Table 1. Effectiveness of the Inactivated SARS-CoV-2 Vaccine Administered at Different Times Close to Virus Challenge^a

	D-3 VP	D0 VP	D1 VP	D2 VP	PBS
Overall severity					
Clinical scores (mean ± SD) ^b	1.3 ± 0.45**	1.1 ± 0.42**	1.69 ± 0.57*	2.17 ± 0.29	2.8 ± 0.57
Body weight loss (%; mean ± SD) ^c	8.89 ± 1.95**	10.02 ± 1.52*	10.17 ± 2.51	10.24 ± 2.91	13 ± 2.45
Lung histology score (mean ± SD)	5.92 ± 1.36**	7.33 ± 1.33*	8.25 ± 0.76	8.67 ± 0.58	8.58 ± 0.92
Viral load (RdRp gene copies/1 e4 β-actin, mean ± SD)	6.76 ± 2.76**	14.56 ± 7.38	8.12 ± 1.72**	15.45 ± 10.01	27.63 ± 12.77
Nasal turbinates	0.66 ± 0.34**	2.48 ± 1.19	3.03 ± 0.04	2.53 ± 1.45	5.56 ± 3.19
Infectious viral titer (LogTCID ₅₀ /ml)	0.59 ± 1.32***	1.08 ± 1.49***	0.74 ± 1.23***	1.8 ± 1.58*	4.29 ± 0.41
Lung antigen expression	0.49 ± 1.09***	3.86 ± 0.24*	4.24 ± 0.23**	4.78 ± 0.26	4.96 ± 0.24
Lung antigen expression	+	++	++	+++	+++
Intestine					
Inflammatory damage ^e	+	+	++	+++	+++
Antigen expression ^f	+	+	++	++	+++
Serum antibody (Geometric mean ± SEM)					
IgG-RBD	696.4 ± 293.9**	174.1 ± 20**	70.7 ± 22.36	58.5 ± 33.33	<100 ^g
IgG-N	229.7 ± 40**	114.9 ± 20**	100 ± 0**	100 ± 0*	<100
Neutralizing antibody	91.9 ± 24**	11.5 ± 3.72*	<5	<5	<5 ^g

Abbreviations: N, nucleocapsid protein; RBD, receptor-binding domain; RdRp, RNA-dependent RNA polymerase; TCID₅₀, 50% tissue culture infectious doses.^a All data represent 4 dpi^b A score of 1 was given to each of the following clinical signs: lethargy, ruffled fur, hunchback posture, and rapid breathing.^c Body weight at 4 dpi minus 0 dpi body weight^d +, bronchioles and a few foci of alveoli; ++ bronchioles and patchy areas of alveoli; +++ diffuse alveoli affecting all the lobes examined^e +, intestinal lamina propria infiltration; ++ intestinal lamina propria infiltration and edema; +++ intestinal lamina propria infiltration, edema and destruction of intestinal villi^f +, N protein expressing enterocytes were less frequent; ++ N protein expressing enterocytes were frequently found but with lower expression intensity; +++ N protein expressing enterocytes were frequently found with high expression intensity

N/D not determined

^g Serum samples dilution started at 1:100 for ELISA assay, 1:5 for microneutralization assay, respectively* $P < .05$, ** $P < .01$, *** $P < .001$, **** $P < .0001$ when compare to SARS-CoV-2 infection without vaccination.

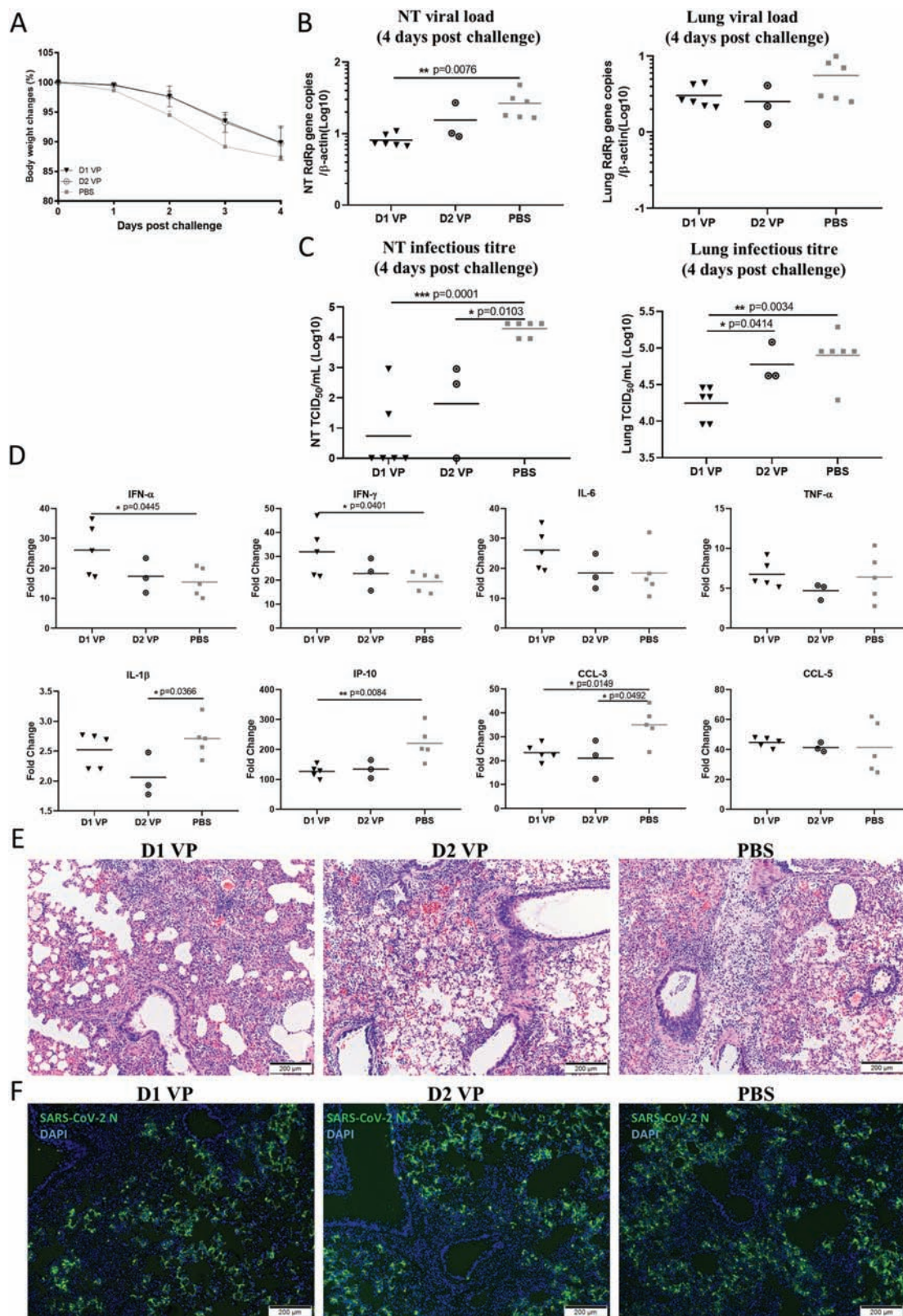
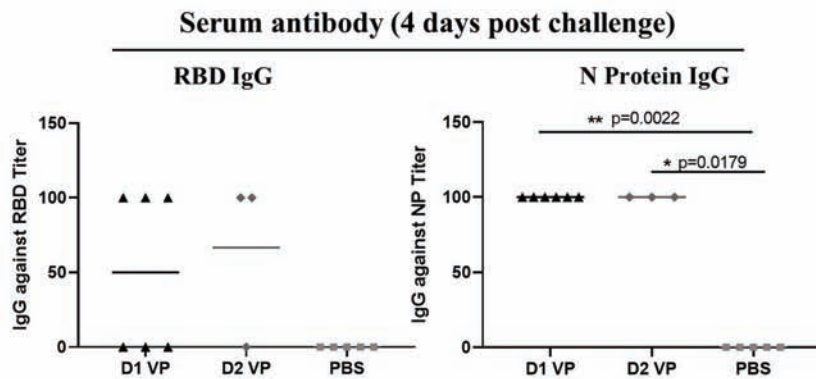
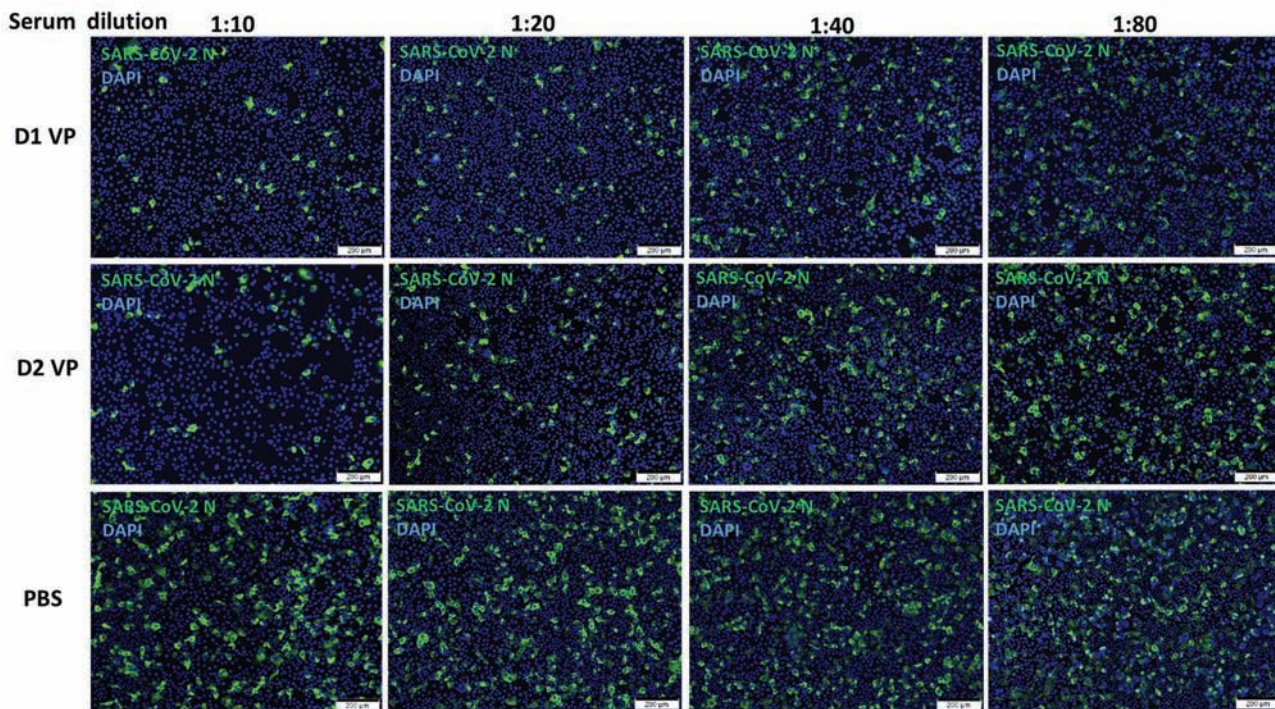


Figure 5. The outcomes of the hamsters that received vaccination shortly after virus challenge. The outcomes of the hamsters that received 1 dose of vaccine at 1 or 2 days post virus challenge (indicated as D1 VP and D2 VP, respectively). **A.** Body weight changes of the hamsters up to 4 days post-virus challenge. $n = 6$ each for the D1 VP and PBS control groups, $n = 3$ for the D2 VP group. **B.** The viral load in the hamsters' nasal turbinate (left panel) and lung (right panel) tissues at 4 dpi were determined by qRT-PCR. $n = 6$ each for the D1 VP and PBS groups, $n = 3$ for the D2 VP group. The error bars indicated standard deviations. P values were calculated by one-way ANOVA. **C.** Infectious viral

G



H



I

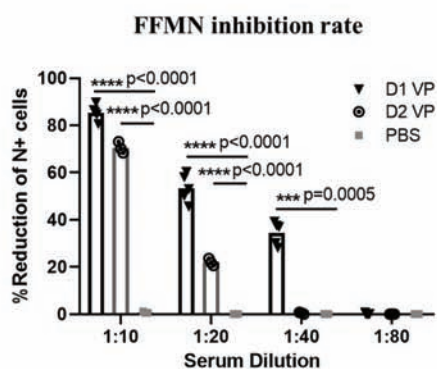


Figure 5. Continued.

titers in the nasal turbinate (left panel) and lung (right panel) tissues at 4 dpi were determined by TCID₅₀ assay in Vero E6 cells. n = 6 each for the D1 VP and PBS control groups, n = 3 for the D2 VP group. The error bars indicated standard deviations. *P* values were calculated by one-way ANOVA. *D*. Gene expression profile of inflammatory cytokines/chemokines in the lung tissues of the hamsters at 4 dpi determined by qRT-PCR. The relative expression levels of each gene compared to mock-infected hamsters were shown. n = 3 to 5 for each group. The error bars indicated standard deviations. *P* values were calculated by Student's *t*-test. *E*. Representative H&E-stained images of

or isotypic switching were likely suboptimal. Despite the occurrence of pneumonia after wild-type virus challenge, the disease was not more severe and no excess eosinophilic infiltration was observed as previously reported in formalin-inactivated whole virion vaccination for measles and respiratory syncytial virus. Thus, inactivated SARS-CoV-2 vaccines should generally be safe even if vaccinated individuals are exposed to the wild-type virus shortly before or after vaccination, a situation which is quite likely to occur when a huge vaccination campaign is held during a pandemic. The detectable protection by vaccine given 3 days before to 2 days after virus challenge is not completely unexpected. We have previously shown that mice vaccinated with monovalent subunit influenza A H1N1 2009 vaccine 3 days before wild-type virus challenge can improve survival with earlier onset of virus neutralizing antibody [30]. Furthermore, the high enough virus inoculum to ensure severe pneumonia in hamster may not happen in the patient situation. Thus, a low degree of immune protection rendered by vaccines given around the time of virus exposure could still be clinically relevant.

While the induction of some immune protection in D-3 vaccinated hamsters is not surprising, the significant reduction of clinical severity score and viral load in nasal turbinates or lungs at D0, D1, and even D2 vaccinated hamster is rather unexpected. Studies of postexposure vaccination generally showed that this approach works in virus infections with long incubation periods when the vaccine stimulates protective immune responses through another route which is faster or stronger than that provoked by the natural infection route. Thus, postexposure vaccination is effective in hepatitis A and B, measles, chickenpox, and mumps, which have mean incubation periods of over 10 days [31].

Nonspecific stimulation of the innate immune system, or epigenetic reprogramming of innate immune cells which has been termed “trained immunity” may have contributed to the protection of hamsters by our inactivated whole virion SARS-CoV-2 vaccine. Trained immunity suggested that whole microbe vaccines, such as BCG or measles-mumps-rubella vaccines, can stimulate innate immune cells to provide nonspecific protection independently of lymphocytes [32]. The presence of detectable antibodies by FFMN assay in the D1 and D2 vaccine group,

but not the PBS group, is suggestive of an adaptive immune response triggered by the vaccine rather than by virus challenge.

Though the induction of innate and adaptive immune responses with robust protection against virus challenge after vaccination against inactivated whole virion SARS-CoV-2 vaccine were reported, only mild clinical disease and pathology could be achieved in unvaccinated controls. Moreover, only rhesus macaques with advanced age were associated with more severe radiological and histopathological changes [33]. At least 2 other groups have evaluated their inactivated whole virion SARS-CoV-2 vaccines by the conventional immunization regimen in the hamster model, which is more available and less expensive [34, 35]. Thus it is reasonable to investigate by this hamster model vaccinated by this unconventional regimen to exclude the possibility of vaccine-enhanced diseases.

In summary, inactivated whole virion SARS-CoV-2 vaccine did not trigger vaccine-enhanced disease in our hamster model, even when the vaccine is given within a short period before or after exposure to the wild-type virus. Moreover, the vaccine still gives some protection to immunized animals especially when given at D-3 or D0. Further studies should be performed to understand differences between responses to inactivated SARS-CoV-2 and paramyxovirus (measles, RSV) vaccines. The findings of our study are limited to inactivated whole virion vaccines in hamsters. Cell-mediated immune responses cannot be studied due to the lack of hamster-biomarker specific antibodies. Further studies with other vaccine platforms in other mammalian models are warranted.

Supplementary Data

Supplementary materials are available at *Clinical Infectious Diseases* online. Consisting of data provided by the authors to benefit the reader, the posted materials are not copyedited and are the sole responsibility of the authors, so questions or comments should be addressed to the corresponding author.

Notes

Disclaimer. The funding sources had no role in the study design, data collection, analysis, interpretation or writing of the paper.

Financial Support. This study was partly supported by the Health and Medical Research Fund (COVID190123) of the Food and Health Bureau, Hong Kong Special Administrative Region Government, and donations from Lee Wan Keung Charity Foundation Limited, Richard Yu and Carol

histopathological changes in the hamsters' lung tissues at 4 dpi. No obvious differences in the lung histopathological changes were observed among the vaccinated hamsters (D1 VP or D2 VP) and the PBS control hamsters. Scale bars = 200 μ m. *F*. Immunofluorescence-stained images of viral N protein in the hamsters' lung tissues at 4 dpi. The level and distribution of SARS-CoV-2 N protein expression among the lung tissues of the vaccinated hamsters (D1 VP or D2 VP) and the PBS control hamsters are similar. Scale bars = 200 μ m. *G*. Serum IgG titer against RBD (left panel) and N protein (right) at 4 dpi by enzyme immunoassay. $n = 3$ to 6 for each group. The error bars indicated standard deviations. *P* values were calculated by Mann-Whitney test. *H*. Representative immunofluorescence-stained images of SARS-CoV-2 N protein in FFMN assay using Vero E6 cells. SARS-CoV-2 (MOI = 0.1) was allowed to react with the diluted sera obtained from the hamsters vaccinated at D1 or D2, or PBS control hamsters for 1 hour at 37°C before being added to Vero E6 cells. The cells were then fixed and stained for SARS-CoV-2 N protein after 6 hours of incubation. *I*. The percentage of reduction in viral N-positive cells by vaccinated hamsters' sera versus PBS control hamster sera in FFMN assay. $n = 3$ to 6 for each group. *P* values were calculated by Student's *t*-test. Abbreviations: CCL3, chemokine (C-C motif) ligand 3; CCL5, chemokine (C-C motif) ligand 5; DAPI, 4',6-diamidino-2-phenylindole; dpi, day post virus challenge; IFN- α , interferon alpha; IFN- γ , interferon gamma; IL-1 β , interleukin 1 beta; IL-6, interleukin 6; IP-10, interferon gamma induced protein 10; N, SARS-CoV-2 nucleocapsid protein; NT, nasal turbinate; RdRp, SARS-CoV-2 RNA-dependent RNA polymerase; TNF- α , tumour necrosis factor alpha; VP, inactivated SARS-CoV-2 whole virion vaccine.

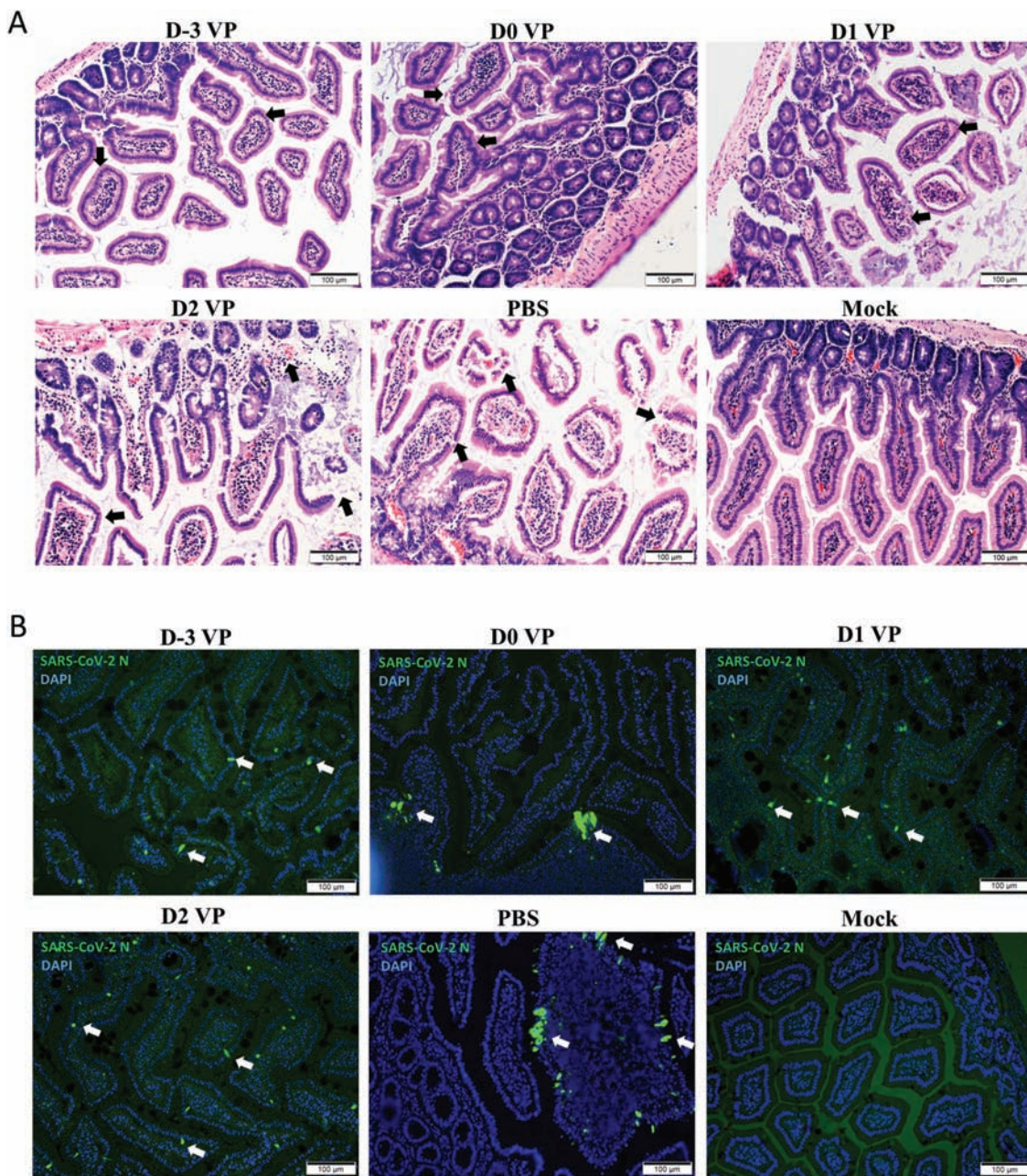


Figure 6. Histopathological changes of the intestines of the hamsters vaccinated shortly before or after virus challenge at 4 dpi. *A.* Representative H&E-stained images of the hamsters' small intestine sections. The intestines of the D-3 and D0 vaccinated hamsters (D-3 VP and D0 VP) showed mild inflammatory infiltration at the lamina propria and relatively preserved morphology of the intestinal villi (arrows). The intestines of the PBS control hamsters showed severe edema and marked inflammatory cell infiltration at the lamina propria. The intestinal villi were deformed (solid arrows). Less edema was observed in the intestines of D1 and D2 vaccinated hamsters (D1 VP and D2 VP, arrows). Scale bars = 100 µm. *B.* Representative immunofluorescence-stained images of viral N protein expression in the intestinal tissues of the hamsters. In the intestines of the PBS control hamsters, viral N protein-expressing enterocytes were readily found (arrows). In contrast, in the intestines of the D1 and D2 vaccinated hamsters, viral N protein expression was less intense and less diffuse. In the intestines of the D-3 and D0 vaccinated hamsters (arrows), viral N protein expression was even less frequently observed. Scale bars = 100 µm. Abbreviations: DAPI, 4', 6-diamidino-2-phenylindole; N, SARS-CoV-2 nucleocapsid protein; PBS, phosphate-buffered saline; VP, inactivated SARS-CoV-2 whole virion vaccine.

Yu, the Shaw Foundation of Hong Kong, Michael Seak-Kan Tong, May Tam Mak Mei Yin, Hong Kong Sanatorium & Hospital, Hui Ming, Hui Hoy and Chow Sin Lan Charity Fund Limited, Chan Yin Chuen Memorial Charitable Foundation, Marina Man-Wai Lee, the Hong Kong Hainan Commercial Association South China Microbiology Research Fund, the Jessie and George Ho Charitable Foundation, Perfect Shape Medical Limited, Kai Chong Tong, Foo Oi Foundation Limited, Tse Kam Ming Laurence, Betty Hing-Chu Lee, Ping Cham So, and Lo Ying Shek Chi Wai Foundation.

Potential conflicts of interest. J. F.-W. Chan has received travel grants from Pfizer Corporation Hong Kong and Astellas Pharma Hong Kong Corporation Limited, and was an invited speaker for Gilead Sciences Hong Kong Limited and Luminex Corporation. The other authors declared no conflict of interests. The funding sources had no role in study design, data collection, analysis or interpretation or writing of the report. All authors have submitted the ICMJE Form for Disclosure of Potential Conflicts of Interest. Conflicts that the editors consider relevant to the content of the manuscript have been disclosed.

References

- World Health Organization. Weekly epidemiological update - 5 January 2021. Available at: <https://www.who.int/publications/m/item/weekly-epidemiological-update---5-january-2021>. Accessed 11 January 2021.
- To KK, Tsang OT, Leung WS, et al. Temporal profiles of viral load in posterior oropharyngeal saliva samples and serum antibody responses during infection by SARS-CoV-2: an observational cohort study. *Lancet Infect Dis* **2020**; 20:565–74.
- Hung IF, Cheng VC, Li X, et al. SARS-CoV-2 shedding and seroconversion among passengers quarantined after disembarking a cruise ship: a case series. *Lancet Infect Dis* **2020**; 20:1051–60.
- Li X, Sridhar S, Chan JF-W. The Coronavirus Disease 2019 pandemic: how does it spread and how do we stop it? *Curr Opin HIV AIDS* **2020**; 15:328–35.
- Chan JF, Zhang AJ, Yuan S, et al. Simulation of the clinical and pathological manifestations of Coronavirus Disease 2019 (COVID-19) in golden Syrian hamster model: implications for disease pathogenesis and transmissibility. *Clin Infect Dis* **2020**; 71:2428–46.
- World Health Organization. Coronavirus disease 2019 (COVID-19) Situation Report – 46. Available at: https://www.who.int/docs/default-source/coronaviruse/situation-reports/20200306-sitrep-46-covid-19.pdf?sfvrsn=96b04ad4_4. Accessed 11 January 2021.
- Consortium WHOIST, Pan H, Peto R, et al. Repurposed antiviral drugs for Covid-19 - interim WHO solidarity trial results. *N Engl J Med* **2020**; 382:1787–99.
- Hung IF, Lung KC, Tso EY, et al. Triple combination of interferon beta-1b, lopinavir-ritonavir, and ribavirin in the treatment of patients admitted to hospital with COVID-19: an open-label, randomised, phase 2 trial. *Lancet* **2020**; 395:1695–704.
- Chen P, Nirula A, Heller B, et al; BLAZE-1 Investigators. SARS-CoV-2 neutralizing antibody LY-CoV555 in outpatients with Covid-19. *N Engl J Med* **2021**; 384:229–37.
- Group A-TL-CS, Lundgren JD, Grund B, et al. A neutralizing monoclonal antibody for hospitalized patients with Covid-19. *N Engl J Med* **2020**. doi:10.1056/NEJMoa2033130
- Simonovich VA, Burgos Pratz LD, Scibona P, et al. A randomized trial of convalescent plasma in Covid-19 severe pneumonia. *N Engl J Med* **2020**. doi:10.1056/NEJMoa2031304
- Libster R, Perez Marc G, Wappner D, et al. Early high-titer plasma therapy to prevent severe Covid-19 in older adults. *N Engl J Med* **2021**. doi:10.1056/NEJMoa2033700
- Cheng VC, Wong SC, Chuang VW, et al. The role of community-wide wearing of face mask for control of coronavirus disease 2019 (COVID-19) epidemic due to SARS-CoV-2. *J Infect* **2020**; 81:107–14.
- Lee WS, Wheatley AK, Kent SJ, DeKosky BJ. Antibody-dependent enhancement and SARS-CoV-2 vaccines and therapies. *Nat Microbiol* **2020**; 5:1185–91.
- Gao Q, Bao L, Mao H, et al. Development of an inactivated vaccine candidate for SARS-CoV-2. *Science* **2020**; 369:77–81.
- van Doremalen N, Lambe T, Spencer A, et al. ChAdOx1 nCoV-19 vaccine prevents SARS-CoV-2 pneumonia in rhesus macaques. *Nature* **2020**; 586:578–82.
- Corbett KS, Flynn B, Foulds KE, et al. Evaluation of the mRNA-1273 vaccine against SARS-CoV-2 in nonhuman primates. *N Engl J Med* **2020**; 383:1544–55.
- Acosta PL, Caballero MT, Polack FP. Brief history and characterization of enhanced respiratory syncytial virus disease. *Clin Vaccine Immunol* **2015**; 23:189–95.
- Polack FP. Atypical measles and enhanced respiratory syncytial virus disease (ERD) made simple. *Pediatr Res* **2007**; 62:111–5.
- Liu L, Wei Q, Lin Q, et al. Anti-spike IgG causes severe acute lung injury by skewing macrophage responses during acute SARS-CoV infection. *JCI Insight* **2019**; 4:e123158.
- Mok BW-Y, Cremin CJ, Lau S-Y, et al. SARS-CoV-2 spike D614G variant exhibits highly efficient replication and transmission in hamsters. *bioRxiv* **2020**:2020.08.28.271635.
- Chu H, Chan JF, Yuen TT, et al. Comparative tropism, replication kinetics, and cell damage profiling of SARS-CoV-2 and SARS-CoV with implications for clinical manifestations, transmissibility, and laboratory studies of COVID-19: an observational study. *Lancet Microbe* **2020**; 1:e14–23.
- Li C, To KKW, Zhang AJX, et al. Co-stimulation with TLR7 agonist imiquimod and inactivated influenza virus particles promotes mouse B cell activation, differentiation, and accelerated antigen specific antibody production. *Front Immunol* **2018**; 9:2370.
- Chan JF-W, Yuan S, Zhang AJ, et al. Surgical mask partition reduces the risk of noncontact transmission in a golden Syrian hamster model for coronavirus disease 2019 (COVID-19). *Clin Infect Dis* **2020**; 71:2139–49.
- Zhang AJ, Lee AC-Y, Chu H, et al. Severe acute respiratory syndrome coronavirus 2 infects and damages the mature and immature olfactory sensory neurons of hamsters. *Clin Infect Dis* **2021**; 73:e503–12.
- Lee AC, Zhang AJ, Chan JF, et al. Oral SARS-CoV-2 inoculation establishes sub-clinical respiratory infection with virus shedding in golden Syrian hamsters. *Cell Rep Med* **2020**; 1:100121.
- Zhang AJ, Lee AC, Chan JF, et al. Co-infection by severe acute respiratory syndrome coronavirus 2 and influenza A(H1N1)pdm09 virus enhances the severity of pneumonia in golden Syrian hamsters. *Clin Infect Dis* **2021**; 72:e978–92.
- Lee ACY, Zhu HS, Zhang AJX, et al. Suboptimal humoral immune response against influenza A(H7N9) virus is related to its internal genes. *Clin Vaccine Immunol* **2015**; 22:1235–43.
- Katzelnick LC, Gresh L, Halloran ME, et al. Antibody-dependent enhancement of severe dengue disease in humans. *Science* **2017**; 358:929–32.
- Zhang AJ, Li C, To KK, et al. Toll-like receptor 7 agonist imiquimod in combination with influenza vaccine expedites and augments humoral immune responses against influenza A(H1N1)pdm09 virus infection in BALB/c mice. *Clin Vaccine Immunol* **2014**; 21:570–9.
- Gallagher T, Lipsitch M. Postexposure effects of vaccines on infectious diseases. *Epidemiol Rev* **2019**; 41:13–27.
- Netea MG, Joosten LA, Latz E, et al. Trained immunity: a program of innate immune memory in health and disease. *Science* **2016**; 352:aaf1098.
- Muñoz-Fontela C, Dowling WE, Funnell SGP, et al. Animal models for COVID-19. *Nature* **2020**; 586:509–15.
- Ragan I, Hartson L, Dutt T, et al. A whole virion vaccine for COVID-19 produced via a novel inactivation method: results from animal challenge model studies. *bioRxiv* **2020**.
- Mohandas S, Yadav PD, Shete-Aich A, et al. Immunogenicity and protective efficacy of BBV152, whole virion inactivated SARS-CoV-2 vaccine candidates in the Syrian hamster model. *iScience* **2021**; 24:102054.